



# A Reusable Behavior of Ruthenium Oxide-PtNP-Nafion Metal Nano Composite Towards Glucose Biosensing

Shankara Narayanan Jeyaraman

Plant Head, Accurex Biomedical Pvt. Ltd.

Received: 05<sup>th</sup> January, 2024; Revised: 10<sup>th</sup> February, 2024; Accepted: 09<sup>th</sup> March, 2024; Available Online: 05<sup>th</sup> April, 2024

## ABSTRACT

This study introduces a novel composite (RuO<sub>2</sub>-PtNP-N) for non-enzymatic glucose sensing. RuO<sub>2</sub>-PtNP-N is fabricated through electrodeposition of platinum nanoparticles onto a pre-cast RuO<sub>2</sub>-Nafion composite on a glassy carbon electrode. The research demonstrates that RuO<sub>2</sub>-PtNP-N exhibits superior sensitivity compared to RuO<sub>2</sub>-N and Pt-N composites. This enhanced performance is attributed to the favorable orientation of PtNPs within the porous RuO<sub>2</sub> matrix. Various characterization techniques, including cyclic voltammetry, chronoamperometry, and spectroscopic methods, were employed to analyze the sensor's electrochemical properties and surface characteristics. The RuO<sub>2</sub>-PtNP-N sensor displayed a linear response up to 24 mM glucose with a sensitivity of 0.328 mA mM<sup>-1</sup> cm<sup>-2</sup>. Furthermore, the sensor exhibited good reproducibility over a 41-day period, indicating excellent surface stability. Additionally, the sensor demonstrated high selectivity for glucose in the presence of potential interfering species. The determination of glucose in serum samples highlights the sensor's promising potential for practical applications.

**Keywords:** Glucose sensor, Non-enzymatic, Ruthenium oxide, Platinum nanoparticles, Nafion.

International Journal of Health Technology and Innovation (2024)

**How to cite this article:** Jeyaraman SN. A Reusable Behavior of Ruthenium Oxide-PtNP-Nafion Metal Nano Composite towards Glucose Biosensing. International Journal of Health Technology and Innovation. 2024;3(1):15-20.

**Doi:** 10.60142/ijhti.v3i01.04

**Source of support:** Nil.

**Conflict of interest:** None

## INTRODUCTION

The accurate and selective detection of glucose has been crucial for clinical diagnosis, food industries, pharmacy, and environmental monitoring for over two decades.<sup>1-6</sup> Numerous studies have explored enzyme-based catalysts, particularly glucose oxidase (GOD), for glucose oxidation.<sup>7</sup> However, the performance of these sensors is hampered by enzyme instability under current environmental conditions and the adsorption of blood proteins. Furthermore, sensor fabrication using GOD immobilization is susceptible to various environmental factors like solution pH, humidity, presence of toxic chemicals, and temperature.<sup>8</sup> Enzyme-dependent sensors often suffer from poor reproducibility and inadequate long-term stability due to enzyme degradation during immobilization.<sup>9</sup> A significant drawback of enzyme-based electrodes is the interference from other oxidizable species in blood samples, such as ascorbic acid and uric acids, which significantly affect glucose detection.

In contrast, non-enzymatic electrochemical glucose sensors, which generate an electrical current by directly oxidizing glucose on the electrode surface, have attracted

considerable interest.<sup>10,11</sup> Recent research has explored various methods for glucose concentration detection, including electrochemical, colorimetric, piezoelectric, and thermoelectric biosensors.<sup>12-16</sup> Among these, electrochemical biosensors have been widely used, but most rely on enzymes.<sup>17-20</sup>

Previous studies have reported on the use of various metal nanoparticles (Au, Pt, Co, Cu, Ni, Co<sub>3</sub>O<sub>4</sub>, NiO, WO<sub>3</sub>, RuO<sub>2</sub>, etc.) for direct glucose oxidation<sup>21-23</sup>. Due to the easy corrosion of Ni, Cu, and Co in highly alkaline media and the conversion of Pt to poorly conducting oxides, noble metals like Ru and Ir are preferred for sensing organic compounds due to their high ohmic conductivity and chemical and thermal stability.<sup>24</sup> RuO<sub>2</sub>, extensively studied in chlorine evolution for chlor-alkali industries, also finds applications as a photocatalyst for water reduction and the electro-oxidation of ethanol, methanol, benzyl alcohol, and catechol.<sup>25-27</sup> Compared to bulk electrodes, RuO<sub>2</sub> electrodes modified with these materials exhibit unique characteristics such as a high surface area-to-volume ratio, promoting rapid mass transport, good electrocatalytic activity, and biocompatibility.<sup>26</sup>

Noble metal nanoparticles (NPs) have emerged as attractive materials for glucose biosensor development due to their unique physicochemical properties. These NPs possess excellent electrical conductivity, facilitating efficient electron transfer during the biosensing process.<sup>28,29</sup> Additionally, their inherent catalytic properties enhance the rate of the enzymatic reaction between glucose and the biosensor. Notably, the large surface area offered by NPs provides a superior platform for biomolecule adsorption, including glucose. Among various noble metals, platinum nanoparticles (PtNPs) have been extensively studied and established as prominent candidates for glucose biosensor applications. PtNPs exhibit exceptional electrocatalytic behavior towards glucose oxidation, by providing high electron transfer rate. Furthermore, their biocompatibility and high conductivity make them suitable for potential *in-vivo* applications.<sup>30-33</sup>

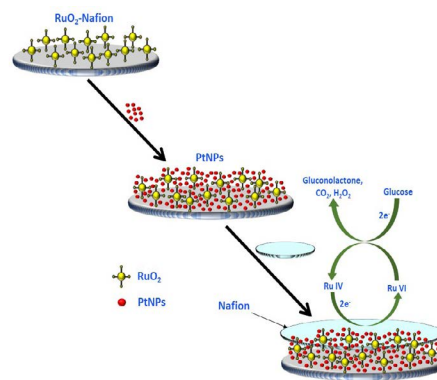
This research introduces a straightforward method for creating a sensor (RuO<sub>2</sub>-PtNP-N electrode) that detects glucose. The technique combines two approaches: drop casting and electrochemistry. Unlike traditional sensors that use enzymes, this one relies on a direct chemical reaction between glucose and the electrode surface at a specific voltage (0.2 V compared to a silver/silver chloride reference electrode).

## Experimental

### Materials and Apparatus

N,N-diethyl-N-methyl-N-(2-methoxyethyl) ammoniumtetrafluoroborate (DEMEBF<sub>4</sub>) Kanto Chemical Co, Japan. Absolute ethanol 99.9% was procured from S.D. Fine-Chemical Limited, India. Zero-grade nitrogen was obtained from Sigma Gases & Services, India. Ruthenium (IV) oxide, Potassium hexachloroplatinate (IV), Nafion perforated solution (5%), Analytical grade NaOH, NaCl, KCl, Na<sub>2</sub>HPO<sub>4</sub>, NaH<sub>2</sub>PO<sub>4</sub>, D-glucose, fructose, L-dopa, sucrose, catechol, uric acid, ascorbic acid, sulphuric acid, ferrocene and ethanol were purchased from Sigma Aldrich, USA. All the experiments were carried out using De-ionized water of conductivity 0–0.5 S/m purified with a Glen RO+ system was obtained from Glen India Limited. Phosphate buffer (0.1 M; pH 7.4) containing NaCl (10 mM), NaH<sub>2</sub>PO<sub>4</sub> (100 mM), and KCl (2.7 mM) was used for glucose sensing.

The electrochemical measurements were carried out using Metrohm PSTAT Mini 910 (Switzerland), which has the potential range from -2 to +2 V. A conventional three-electrode system from Gamry Instrument USA, consisting of modified glassy carbon (3mm diameter) as the working, a platinum wire (1 mm diameter) as the counter and Ag/AgCl, as the reference electrodes. PANalytical make X-ray diffractometer from X'Pert PRO that uses source Cu K (2.2 kW max) from UK and FTIR from Bruker Optic GmbH (model no. Sensor 27) were utilized for acquiring FTIR spectra, from USA. Micro-Raman measurements were recorded using imaging spectrograph STR 500 mm focal length laser Raman spectrometer, from Japan. Ultraviolet Visible (UV-vis) spectra were measured



**Scheme 1.** RuO<sub>2</sub>-PtNP-Nafion mediated electro oxidation of glucose

using PerkinElmer-Lambda 35 from USA, in the range 190 to 400 nm.

## RESULTS AND DISCUSSION

### Formation of RuO<sub>2</sub>-PtNP-Nafion Composite on Glassy Carbon Electrode

Glassy carbon (GC) surface was polished using emery paper (no. 800, Carborundum Universal, India) and cleaned with 20% HCl for 20 minutes and dried. Then 4 mg of RuO<sub>2</sub> was mixed in 10  $\mu$ L of 1% nafion. Uniform distribution was attained by sonicating the mixture for 30 minutes, 5  $\mu$ L of the sonicated mixture was drop casted on the GC surface and dried at room temperature for 30 minutes. Then the RuO<sub>2</sub>-nafion modified electrode was then electrodeposited with PtNPs. Platinum nano particle was electrodeposited on the GC electrodes by applying a potential of -2.0 V vs Ag/AgCl in N<sub>2</sub> saturated DEMEBF<sub>4</sub> containing 35 mM K<sub>2</sub>PtCl<sub>6</sub>. The PtNPs modified RuO<sub>2</sub>-Nafion electrode was then electrochemically cleaned by scanning the electrode at the potential between -0.2 and +1.5 V vs Ag/AgCl repeatedly on scan rate of 500 mVs<sup>-1</sup> for 10 minutes in 0.5 M H<sub>2</sub>SO<sub>4</sub> aqueous solution under a N<sub>2</sub> gas atmosphere.<sup>34</sup>

### Characterization of the RuO<sub>2</sub>-PtNP-N

The XRD, FT-IR, UV, Raman spectra of (curve a) RuO<sub>2</sub>, (curve b) PtNPs, (c) RuO<sub>2</sub>-PtNPs-Nafion are illustrated in Figure 1. In the XRD (Figure 1 A, a), two major peaks at 2 $\theta$  28.0 and 35.01 are assigned to the diffraction from the (110) and (101) planes of tetragonal rutile phase for RuO<sub>2</sub> (JCPDS powder diffraction pattern: 00-040-1290). The diffraction planes (111) at 40.00 $^{\circ}$  was observed for PtNPs (Figure 1 A, b). In Figure 1 A, c, the diffraction patterns at (110) 27.90 $^{\circ}$  RuO<sub>2</sub>, (111) 40.00 $^{\circ}$  PtNPs, for RuO<sub>2</sub> indicates the presence of RuO<sub>2</sub> and PtNPs in the same composite.

The FTIR (Figure 1 B, a) band at 474 cm<sup>-1</sup> indicates the presence of RuO<sub>2</sub>. For PtNPs a broad hump at 570 cm<sup>-1</sup> was observed (Figure 1 B, b). In the case of RuO<sub>2</sub>-PtNPs-Nafion nano composite (Figure 1 B, c) metallic peaks at 600 and 700 cm<sup>-1</sup> for RuO<sub>2</sub> and PtNPs were clearly seen. Multiple peaks at 1200 to 1400 cm<sup>-1</sup> corresponds to the C-OH bending motion and 1618 cm<sup>-1</sup> for O-H stretching vibrations are seen due to the presence of nafion in the nanocomposite.

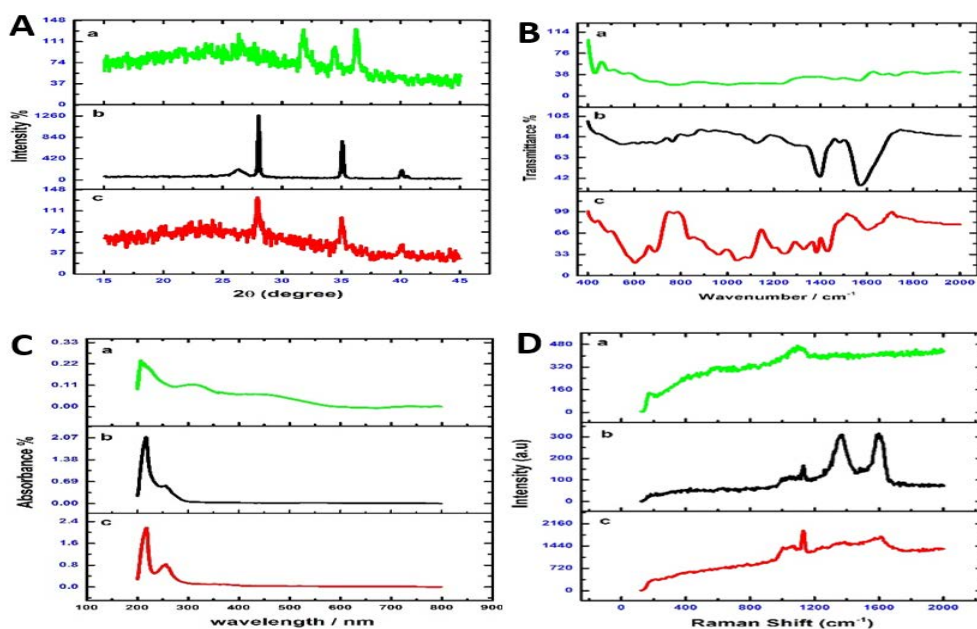


**Figure 1:** (A) XRD, (B) FT-IR (C) UV and (D) Raman spectra data of RuO<sub>2</sub> (curve a), PtNPs (curve b), RuO<sub>2</sub>- PtNPs-Nafion (curve c)

The UV absorption peak (Figure 1 C, a) at 462 nm corresponds to the presence of Ru metal ions. A sharp UV peak at 200 nm was observed for PtNPs modified electrode (Figure 1 C, B). In the case of RuO<sub>2</sub>-PtNPs nano composite (Figure 1 C), a sharp peak at 200 nm for RuO<sub>2</sub> and a little hump at around 370 nm for PtNPs were observed. It is to note that the peak for PtNPs was shifted towards the negative direction (Figure 1 C) because of the effective formation of the nano composite.

Micro-Raman spectra of the RuO<sub>2</sub>-Nafion, PtNPs and RuO<sub>2</sub>-PtNPs-Nafion composites are shown in Figure 3 D.

RuO<sub>2</sub> has a tetragonal structure with 15 modes of optical phonons, three of which are Raman-active within the range 400 to 800 cm<sup>-1</sup>.<sup>35</sup> As shown from Figure 1 A, C and D, a little hump at 200 cm<sup>-1</sup> followed by noisy humps at 400 cm<sup>-1</sup> indicates the presence of RuO<sub>2</sub>. And for PtNPs a broad hump at 1000 cm<sup>-1</sup> and two sharp peaks at 1360 and 1600 cm<sup>-1</sup> were observed.<sup>36</sup> As seen, the RuO<sub>2</sub> and characteristic peaks at 200, 1000, 1360 and 1600 cm<sup>-1</sup> were observed (Figure 1 C and D) for RuO<sub>2</sub>-PtNP-Nafion nano composite.

### Electrochemical Cyclic Voltammetric Analysis of RuO<sub>2</sub>-PtNP-Nafion

Comparative CV behaviors of the RuO<sub>2</sub>-Nafion (curve a and b), PtNP-Nafion (curve b,c) and RuO<sub>2</sub>-PtNP-Nafion (curve e and f) composites in 0.1 M PBS in the presence (solid line) and the absence of (dotted line) 1-mM glucose are shown in Figure 2. In the presence of glucose, the RuO<sub>2</sub>-PtNP-Nafion surface (Figure 2, curve f) showed large charging (1.035e-4) current compared to the RuO<sub>2</sub>-Nafion (3.656e-5) (Figure 2, curve B) and PtNP-Nafion (6.672e-5) (Figure 2, curve d) modified electrodes. This is related to the large surface area provided by the RuO<sub>2</sub>/PtNP through their functional groups such as hydroxyl, epoxide and carboxyl groups, whereas RuO<sub>2</sub> possess only oxide functional groups.

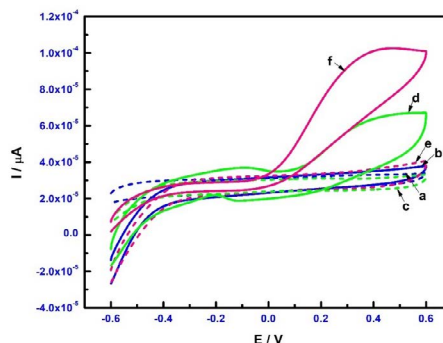


**Figure 2:** CV behaviors of the RuO<sub>2</sub>-Nafion (blue), PtNP (green) and RuO<sub>2</sub>- PtNPs-Nafion (rose), in the absence (dotted line) and presence of (solid line) 1 mM glucose in 0.1 M PBS measured at the scan rate of 50 mV/s.

It is to note that the PtNP-Nafion modified also shown good glucose oxidation current (6.672e-5) compared to the RuO<sub>2</sub>-Nafion composite (3.656e-5) (Figure 2, curve d). This is due to the ability of PtNPs in direct oxidation of glucose reported by our group.<sup>31</sup> On the other hand, the high activity of RuO<sub>2</sub>-PtNP-Nafion in PBS may be related to the structural reorganization and stabilization of metal coordination center due to charge compensation method as presented in Scheme 1. It is clear from the result that the RuO<sub>2</sub> provides extra surface area for the PtNPs to directly react with the glucose molecules. No prominent oxidation peaks were observed in the absence of 1-mM glucose on any of the substrates. Thus, the increased peak current in the presence of 1-mM glucose is directly related to the glucose oxidation by RuO<sub>2</sub>-PtNP-Nafion and PtNP-Nafion substrates.

### Performance Test and Stability

The glucose biosensing temperature and pH of RuO<sub>2</sub>-PtNP-Nafion modified electrode was studied in the presence of 1-mM

glucose in PBS 7.4 (Figure 3 A, B). The operational temperature study experiment was conducted in seven different temperatures (viz. 20, 25, 30, 35, 40, 45 and 50°C) (Figure 3 A) at fixed pH (7.4). The solution temperature was controlled (20–50°C) using a recirculatory. The optimal temperature was observed in the range between 25 to 40°C (Figure 3 A). Though the sensor's biosensing behavior diminished after 45°C. The pH analysis was also performed with 1 mM glucose prepared at different pH ranging from 5 to 10 and the RuO<sub>2</sub>-PtNP-Nafion electrode is amperometrically characterized at 37°C (Figure 3 B). The optimal oxidation current was observed at pH 6.5 to 8, which is slightly higher than the oxidation current generated at pH 5 and 8.5. The result shows that the RuO<sub>2</sub>-PtNP-Nafion electrode exhibited excellent amperometric performance at neutral conditions.

Figure 3 C shows the amperometric current behavior of the RuO<sub>2</sub>-PtNP-Nafion modified electrode measured for 48 days in PBS 7.4 containing freshly prepared 1-mM glucose. The stability experiment was carried out once in 3 days. After every successful measurement, the RuO<sub>2</sub>-PtNP-Nafion electrode is stored in PBS pH 7.4 to avoid surface disorientation/damage. The glucose catalytic current for consecutive 41 days almost remained unchanged showing good reproducible behavior of the RuO<sub>2</sub>-PtNP-Nafion composite. But the current started falling down in the subsequent measurements. This shows that the RuO<sub>2</sub>-PtNP-Nafion composite electrode is highly reproducible.

**Amperometric Determination of Glucose**

Concentration dependence glucose oxidation current of RuO<sub>2</sub>-PtNP-Nafion modified glassy carbon electrode was measured using chrono amperometry (Figure 4 A). All the amperometric measurement was carried out at a fixed potential of 0.4 V. During the measurement, 3 mM glucose was added at regular interval (50s) till the sensor attained saturation. As expected, the peak current increases with increase in the glucose concentration. After the addition of 24 mM glucose,

the RuO<sub>2</sub>-PtNP-Nafion surface gets saturated and the sensors behavior is un-altered for the subsequent addition of glucose. This range pretty much covers blood glucose level for a non-diabetic to high diabetic person (18–432 mg/dl). In addition, the time required to reach 95% of the steady state current after every successful addition of glucose is less than 4 seconds.

A calibration curve was plotted for anodic peak current vs concentration of glucose as shown in Figure 4 B. The result shows a linear dependence with a correlation coefficient of 0.991 in the glucose concentration range of 3 mM to 24 mM. The sensitivity of the RuO<sub>2</sub>-PtNP-Nafion electrode was calculated to be 0.328 mA mM<sup>-1</sup> cm<sup>-2</sup>.

**Interference Effects**

The activity of this sensor in the presence of potential interfering substances was analyzed using chrono amperometry (Figure 5).

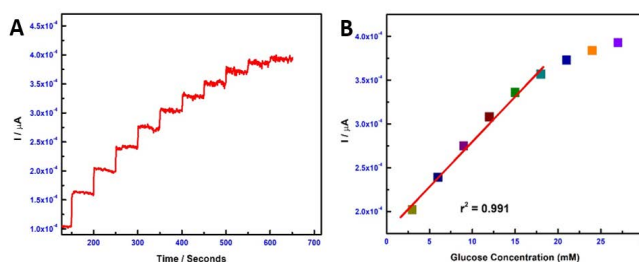


Figure 4: (A) CA behavior of RuO<sub>2</sub>-PtNP-Nafion and (B) Calibration curve of the RuO<sub>2</sub>-PtNP-Nafion

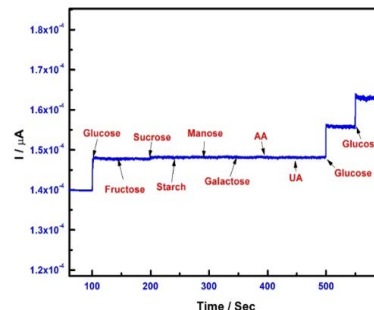


Figure 5: Selective behavior of RuO<sub>2</sub>-PtNP-Nafion towards glucose in PBS (pH 7.4, in presence of other dynamic interfering compounds).

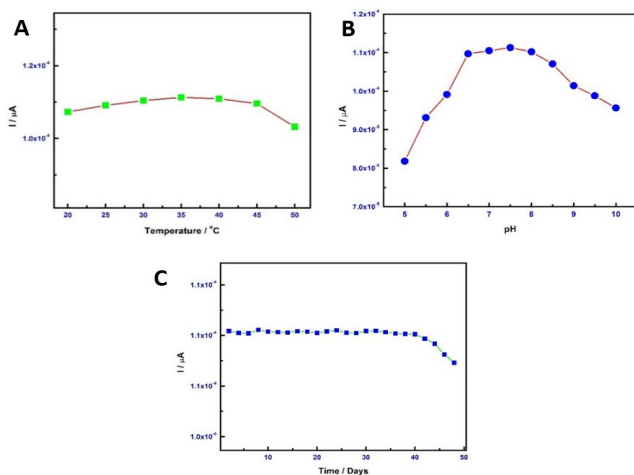


Figure 3: (A) Temperature variation (B) pH variation and (C) Reproducibility analysis of RuO<sub>2</sub>-PtNP-Nafion

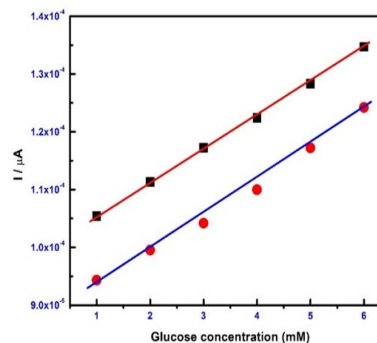


Figure 6: CA behavior of RuO<sub>2</sub>-PtNP-Nafion measured with 1 mM glucose in (a) PBS (7.4) (Black Squares) and (b) Serum (Red round)



The interference species used in this study are ascorbic acid, uric acid, fructose, sucrose, starch, mannose and galactose. In the present study the experiments are carried out by successive addition of 1-mM glucose and interferent species in 0.1 M PBS (pH 7.4). Though ascorbic acid (AA) and uric acid (UA) are normally co-existed interfering compounds other carbohydrates such as sucrose, fructose, galactose, starch, sucrose and mannose are also used in this study to ensure its high selectivity. It is to note that the normal physiological level of glucose in human blood is about 30 times higher than the interfering species such as AA or UA and much higher in food samples. However, it is eliminated from the RuO<sub>2</sub>-PtNP-Nafion composite. As seen from Figure 5, the RuO<sub>2</sub>-PtNP-Nafion composite electrode showed a clear oxidation current after the addition of glucose and no oxidation peaks were observed for other interferent substances. These results confirm high specificity of the RuO<sub>2</sub>-PtNP-Nafion to glucose in presence of common interfering species found in biological and food samples.

### Real Sample Analysis

Figure 6 shows the chrono amperometric glucose oxidation currents measured at an applied potential of 0.4 V vs Ag/AgCl. The black square blocks and the red circle each represent oxidation currents of 1-mM glucose in PBS and 1 mM glucose spiked in serum. As seen from the results plotted in Figure 6, a linear current was observed in both samples after every successful addition of glucose. But the net current in the case of serum spiked sample is 5% less than that of the glucose in PBS. Though the current is linear, the negligible loss of current may be attributed because of presence of blood plasma components which could partially block the contact between glucose and RuO<sub>2</sub>-PtNP metal center. These results still determine that our RuO<sub>2</sub>-PtNP-Nafion composite showed efficient glucose sensing with good recovery in serum sample.

### CONCLUSIONS

This work introduces a novel non-enzymatic glucose sensor comprised of a RuO<sub>2</sub>-PtNP-Nafion composite. This innovative electrode design offers exceptional reproducibility in glucose detection, surpassing conventional methods that often involve intricate and expensive fabrication processes. Notably, the proposed fabrication method is significantly simpler and more cost-effective, eliminating the need for laborious techniques like chemical reduction, thermolysis, and  $\gamma$ -irradiation. The sensor exhibits impressive performance characteristics, boasting high sensitivity (0.328 mA mM<sup>-1</sup> cm<sup>-2</sup>) and remarkable stability over an extended 41-day testing period. Furthermore, the sensor demonstrates excellent selectivity, effectively distinguishing glucose from various interfering species typically present in real-world samples. This enhanced selectivity is attributed to the incorporation of a Nafion layer onto the RuO<sub>2</sub>-PtNP substrate, which significantly improves sensor performance. Finally, the sensor's successful detection of glucose in spiked serum samples underscores its promising potential for practical applications, particularly in implantable

devices for continuous glucose monitoring. This advancement holds significant implications for revolutionizing diabetes management and personalized healthcare strategies.

### REFERENCES

- Galant AL, Kaufman RC, Wilson JD. Glucose: detection and analysis. *Journal of Food Chemistry*. 2015;188:149–160. Available From: doi.org/10.1016/j.foodchem.2015.04.071
- Yoo EH, Lee SY. Glucose biosensors: an overview of use in clinical practice. *Sensors*. 2010;10:4558–4576. Available From: doi.org/10.3390/s100504558
- Amine A, Mohammadi H, Bourais I, Palleschi G. Enzyme inhibition-based biosensors for food safety and environmental monitoring. *Biosensors and Bioelectronics*. 2006; 21(8):1405–1423. Available From: doi.org/10.1016/j.bios.2005.07.012
- Dhara K, Mahapatra DR. Electrochemical nonenzymatic sensing of glucose using advanced nanomaterials. *Microchimica Acta*. 2018;185:1. Available From: doi.org/10.1007/s00604-017-2609-1.
- Terry LA, White SF, Tigwell LJ. The Application of Biosensors to Fresh Produce and the Wider Food Industry. *Journal of Agriculture and Food Chemistry*. 2005; 53:1309–1316. Available From: DOI: 10.1021/jf040319t
- Crouch E, Cowell DC, Hoskins S, Pittson RW, Hart JP. A novel, disposable, screen-printed amperometric biosensor for glucose in serum fabricated using a water-based carbon ink. *Biosensors and Bioelectronics*. 2005;21:712–718. Available From: doi.org/10.1016/j.bios.2005.01.003
- Pankaj M, Bala P, Hunny G, Pravin S. Glucose oxidase-based biosensor for glucose detection from biological fluids. *Sensor Review*. 2020;40/4:497–511. Available From: 10.3390/s100504558
- Valdes TI, Moussy F. In Vitro and In Vivo Degradation of Glucose Oxidase Enzyme Used for an Implantable Glucose Biosensor. *Diabetes Technology & Therapeutics* 2000;2(3):367–376. Available From: 10.1089/15209150050194233.
- Wilson R, Turner APF. Glucose oxidase: an ideal enzyme. *Biosensors and Bioelectronics*. 1992;7:165–185. Available From: doi.org/10.1016/0956-5663(92)87013-F
- Si YT, Choon PT, Enyi Y. Metal nanostructures for non-enzymatic glucose sensing. *Materials Science and Engineering: C*. 2017;70:1018–1030. Available From: doi.org/10.1016/j.msec.2016.04.009
- Hwang DW, Lee S, Seo M, Chung, TD. Recent Advances in Electrochemical Non-enzymatic Glucose Sensors-A Review. *Analytical Chimica Acta*. 2018;1033:1–34. Available From: 10.1016/j.aca.2018.05.051
- Akhtar MA, Batool R, Hayat A, Han D, Riaz S, Khan SU, Nasir M, Nawaz MH, Niu L. Functionalized graphene oxide bridging between enzyme and Au-sputtered screen-printed interface for glucose detection. *ACS Applied Nano Materials*. 2019;2:1589–1596. Available From: 10.1021/acsanm.9b00041
- Tim B, Wolfgang S. Long-term implantable glucose biosensors. *Current Opinion in Electrochemistry*. 2018;10:112–119. Available From: doi.org/10.1016/j.coelec.2018.05.004
- Coyle VE, Kandjani AE, Field MR, Hartley P, Chen M, Sabri YM, Bhargava SK, Co3O4 needles on Au honeycomb as a non-invasive electrochemical biosensor for glucose in saliva. *Biosensors and Bioelectronics*. 2019;141:111479. Available From: doi.org/10.1016/j.bios.2019.111479
- Xiao J, Liu Y, Su L, Zhao D, Zhao L, Zhang X. Microfluidic chip-based wearable colorimetric sensor for simple and facile detection of sweat glucose. *Analytical Chemistry*. 2019;91:14803–

14807. Available From: doi.org/10.1021/acs.analchem.9b03110
16. Han W, He H, Zhang L, Dong C, Zeng H, Dai Y, Xing L, Zhang Y, Xue X, A self-powered wearable noninvasive electronic-skin for perspiration analysis based on piezo-biosensing unit matrix of enzyme/ZnO nanoarrays. *ACS Applied Material Interfaces*. 2017; 9:29526-29537. Available From: 10.1021/acsami.7b07990
  17. Hazhir T, Abbas B, Joseph W. Electrochemical glucose sensors in diabetes management: an updated review (2010–2020), *Chemical Society Review*. 2020;49:7671-7709. Available From: doi.org/10.1039/D0CS00304B
  18. Razia B, Amina R, Mian HN, Akhtar H, Jean LM. A Review of the Construction of Nano-Hybrids for Electrochemical Biosensing of Glucose. *Biosensors*. 2019;9:46. Available From: 10.3390/bios9010046
  19. Liang T, Long Z, Xiaogang G, Xiaoqing M, Chenke Z, Zhuo Z, Yuhuan Z, Fangxin H, Zhisong L, Kanglia T, Chang ML. Rising mesopores to realize direct electrochemistry of glucose oxidase toward highly sensitive detection of glucose. *Advanced Functional Materials*. 2019;44:1903026. Available From: doi.org/10.1002/adfm.201903026
  20. Yoon Y, Lee SN, Shin MK, Kim HW, Choi HK, Lee T, Choi JW. Flexible electrochemical glucose biosensor based on GOx/gold/MoS<sub>2</sub>/gold nanofilm on the polymer electrode. *Biosensors and Bioelectronics*. 2019;140:111343. Available From: 10.1016/j.bios.2019.111343
  21. Wang G, He X, Wang L, Gu A, Huang Y, Fang B, Geng B, Zhang X. Non-enzymatic electrochemical sensing of glucose. *Microchimica Acta*. 2013;180:161–186. Available From: 10.1007/s00604-012-0923-1
  22. Si P, Huang Y, Wang T, Ma J. Nanomaterials for electrochemical non-enzymatic glucose biosensors. *RSC Advance*. 2013;3:3487–3502. Available From: doi.org/10.1039/C2RA22360K
  23. Fleischmann M, Korinek K, Pletcher D. The oxidation of organic compounds at a nickel anode in alkaline solution. *Journal of Electroanalytical Chemistry Interfacial Electrochemistry*. 1971; 31:39–49. Available From: doi.org/10.1016/S0022-0728(71)80040-2
  24. Dharuman V, Pillai KC. RuO<sub>2</sub> electrode surface effects in electrocatalytic oxidation of glucose. *Journal of Solid State Electrochemistry*. 2006;10:967–979. Available From: 10.1007/s10008-005-0033-7
  25. Kumar AS, Pillai KC. Studies of electrochemical behaviour of RuO<sub>2</sub>-PVC film electrodes: dependence on oxide preparation temperature. *Journal of Solid State Electrochemistry*. 2000;4:408–416. Available From: 10.1007/s100089900084
  26. Shankara Narayanan J, Anjalidevi C, Dharman V. Nonenzymatic glucose sensing at ruthenium dioxide–poly(vinyl chloride)–Nafion composite electrode. 2013;17:937–947. 10.1007/s10008-012-1942-x
  27. Jacobs CB, Peairs MJ, Venton BJ. Review: Carbon nanotube based electrochemical sensors for biomolecules, *Analytical Chemical. Acta*. 2010;662:105-127. Available From: 10.1016/j.aca.2010.01.009
  28. Zhao S, Zhang K, Bai, Y, Yang W, Sun C. Glucose Oxidase/ Colloidal Gold Nanoparticles Immobilized in Nafion Film on Glassy Carbon Electrode: Direct Electron Transfer and Electrocatalysis. *Bioelectrochemistry*. 2006; 69:158–163. Available From: doi.org/10.1016/j.bioelechem.2006.01.001
  29. Yang J, Jiang LC, Zhang WD, Gunasekaran SA. Highly Sensitive Non-enzymatic Glucose Sensor based on a Simple Two-step Electrodeposition of Cupric Oxide (CuO) Nanoparticles onto Multiwalled Carbon Nanotube Arrays. *Talanta*. 2010;82:25–33. Available From: 10.1016/j.talanta.2010.03.047
  30. Francisco JF, María IGS, Rebeca JP, Jesús I, Edelmira V. Glucose Biosensor Based on Disposable Activated Carbon Electrodes Modified with Platinum Nanoparticles Electrodeposited on Poly(Azure A). *Sensors*. 2020;20:4489. Available From: doi.org/10.3390/s20164489
  31. Hossain MF, Gymama S. PtNPs decorated chemically derived graphene and carbon nanotubes for sensitive and selective glucose biosensing, *Journal of Electroanalytical Chemistry*. 2020;861:113990. Available From: doi.org/10.1016/j.jelechem.2020.113990
  32. Ankit B, Shankara Narayanan J, Gymama S. Sensitive electrochemical detection of glucose via a hybrid self-powered biosensing system. *Sensing and Bio-Sensing Research*. 2018;20:41–46. Available From: doi.org/10.1016/j.sbsr.2018.08.002
  33. Shankara Narayanan J, Gymama S. Towards a dual in-line electrochemical biosensor for the determination of glucose and hydrogen peroxide. *Bioelectrochemistry*. 2019;128:56–65. Available From: doi.org/10.1016/j.bioelechem.2019.03.005
  34. Da Z, Wan CC, Takeyoshi O, Takeo O. Electrodeposition of Platinum Nanoparticles in a Room-Temperature Ionic Liquid. *Langmuir*. 2011; 27:14662–14668. Available From: doi.org/10.1021/la202992m
  35. Fatima M, Ahcène C, Mohamed J, François M, Abdelaziz K, Mohamed MC. Polyaniline-Grafted RuO<sub>2</sub>-TiO<sub>2</sub>. Heterostructure for the Catalysed Degradation of Methyl Orange in Darkness. *Catalysts*. 2019;9:578. Available From: doi.org/10.3390/catal9070578
  36. Na T, Zhi-You Z, Shi-Gang S, Li C, Bin R, Zhong-Qun T. Electrochemical preparation of platinum nanothorn assemblies with high surface enhanced Raman scattering activity. *Chemical Communication*. 2006;39:4090–4092. Available From: doi.org/10.1039/B609164D